Applied Catalysis B: Environmental 244 (2019) 909–918

Contents lists available at ScienceDirect

Applied Catalysis B: Environmental

journal homepage: www.elsevier.com/locate/apcatb

Insight into the origin of sulfur tolerance of Ag/Al_2O_3 in the H_2-C_3H_6-SCR of NO*x*

Guangyan Xu[a], Jinzhu Ma[a,b,c], Lian Wang[a], Wen Xie[a,c], Jingjing Liu[a,c], Yunbo Yu[a,b,c,*], Hong He[a,b,c,*]

[a] State Key Joint Laboratory of Environment Simulation and Pollution Control, Research Center for Eco-Environmental Sciences, Chinese Academy of Sciences, Beijing, 100085, China
[b] Center for Excellence in Regional Atmospheric Environment, Institute of Urban Environment, Chinese Academy of Sciences, Xiamen, 361021, China
[c] University of Chinese Academy of Sciences, Beijing, 100049, China

ARTICLE INFO

Keywords:
HC-SCR
Ag/Al_2O_3
Sulfur tolerance
DRIFTS-MS
DFT calculations

ABSTRACT

The sulfur tolerance of Ag/Al_2O_3 catalysts in H_2-assisted C_3H_6-SCR was investigated by UV–vis, TPR, TPSR, DRIFTS-MS, and DFT calculations. Ag/Al_2O_3 with higher silver loadings exhibited better deNO*x* performance and sulfur tolerance, especially the 4% Ag/Al_2O_3 catalyst. UV–vis and H_2-TPR revealed that highly dispersed Ag^+ cations were predominant on 2% Ag/Al_2O_3, while more metallic Ag clusters with large sizes were present on the 4% Ag/Al_2O_3. After exposure to SO_2, large amounts of sulfates were adsorbed on the Ag sites and Al sites of the Ag/Al_2O_3 surface. The sulfates were reduced to H_2S and SO_2 in a reducing atmosphere, while they showed little decomposition under real SCR reaction conditions. DRIFTS-MS experiments showed that sulfate species transferred rapidly between Ag sites and Al sites on the Ag/Al_2O_3 catalysts with higher amounts of Ag clusters. DFT calculations revealed that Ag_1 cations show stronger affinity for sulfate species than Ag clusters, thus resulting in blockage by sulfates at the Ag-O-Al interface. Such blocking by sulfates suppressed the activation of C_3H_6 as well as the formation of -NCO species, and thus severely inhibited the deNO*x* performance of 2% Ag/Al_2O_3. In contrast, the rapid mobility of sulfate species on 4% Ag/Al_2O_3 made more active sites available for the formation of key intermediates of HC-SCR, finally contributing to its excellent sulfur tolerance.

1. Introduction

NO*x* emission reduction for diesel engines is an important task for environmental protection. For this application, selective catalytic reduction of NO*x* utilizing on-board diesel or its additives as reductants (HC-SCR) exhibits unique advantages for NO*x* removal compared to the commercial application of NH_3-SCR [1–4]. Among the catalysts employed for the HC-SCR process, alumina-supported silver (Ag/Al_2O_3) is one of the most promising catalysts [4–14]. Moreover, a small amount of hydrogen addition significantly enhances the low-temperature activity of Ag/Al_2O_3 in HC-SCR, which is beneficial for its practical application [15–24].

As diesel engine exhaust contains a certain amount of SO_2, development of catalysts with high sulfur resistance is important for their practical application [1,2,25–27]. Therefore, several researchers have investigated the SO_2 poisoning mechanism of Ag/Al_2O_3 during HC-SCR [28–35]. Generally, the deactivation induced by SO_2 is mainly due to the generation of thermodynamically stable sulfate species, which reduce the active sites available for NO*x* reduction [29,31,32,35]. Meunier et al. [29] found that pretreatment of 1.2% Ag/Al_2O_3 with SO_2 (100 ppm) resulted in rapid and permanent deactivation for C_3H_6-SCR, due to the formation of two sulfate species interacting with Al_2O_3 and silver species, respectively. In contrast, Houel et al. [34] found that sulfur-poisoned 4 wt% Ag/Al_2O_3 could be regenerated in n-octane-SCR at 600 °C. During C_3H_6-SCR at 500 °C, similarly, Park et al. reported that the deNO*x* performance of 2 wt% Ag/Al_2O_3 was completely recovered after the removal of SO_2 [31]. Over an 8 wt% Ag/Al_2O_3 catalyst, interestingly, the addition of SO_2 improved the NO*x* reduction due to the formation of active Ag_2SO_4. Furthermore, the sulfur resistance of Ag/Al_2O_3 is closely related to the nature of the reductant, and oxygenated hydrocarbons were found to be more advantageous for achieving high SO_2 tolerance [32].

Compared with Ag/Al_2O_3, Ag/TiO_2-Al_2O_3 catalysts synthesized by a sol–gel method exhibited superior deNO*x* activity and SO_2 resistance

* Corresponding authors at: State Key Joint Laboratory of Environment Simulation and Pollution Control, Research Center for Eco-Environmental Sciences, Chinese Academy of Sciences, Beijing, 100085, China.
E-mail addresses: ybyu@rcees.ac.cn (Y. Yu), honghe@rcees.ac.cn (H. He).

https://doi.org/10.1016/j.apcatb.2018.11.050
Received 7 September 2018; Received in revised form 10 November 2018; Accepted 17 November 2018
Available online 30 November 2018
0926-3373/

due to a lower rate of sulfate accumulation [36]. Similarly, Umbarkar et al. [33] found that magnesia doping decreased the total acidity of Ag/Al_2O_3 and thus prevented the formation of sulfates, finally contributing to excellent low-temperature catalytic performance and sulfur resistance. Meanwhile, it was reported that H_2 addition improved the SO_2 tolerance of Ag/Al_2O_3 by cleaning off the sulfates adsorbed on silver-containing sites [28,32].

The results mentioned above show that the deactivation of Ag/Al_2O_3 induced by SO_2 is related to the catalyst formulation, gas mixture composition, and reaction temperature [32,33,36,37]. Under real conditions of HC-SCR, the sulfate species were hard to decompose or reduce [29,31,34], while the activity of Ag/Al_2O_3 was completely regenerated once SO_2 was removed [31]. Hence, not only the decomposition and/or reduction behavior of sulfates, but also other factors govern the SO_2 tolerance of Ag/Al_2O_3, which have not yet been fully clarified. To this aim, Ag/Al_2O_3 catalysts were prepared and carefully characterized, and the behaviors of sulfates on the surface of Ag/Al_2O_3 were investigated by TPSR, DRIFTS-MS, and DFT calculations. It was found that sulfate species transferred rapidly at the Ag-O-Al interface of Ag/Al_2O_3 catalysts with greater proportions of Ag clusters, which showed excellent sulfur resistance during H_2-C_3H_6-SCR. This investigation provides a clue for the development of Ag/Al_2O_3 catalysts with excellent sulfur tolerance in HC-SCR.

2. Materials and methods

2.1. Materials and catalytic performance studies

Ag/Al_2O_3 catalysts were prepared by an impregnation method, as reported in our previous works [7,38]. After impregnation, these samples were further calcined in flowing air at 600 °C for 3 h. A sample with x wt% silver loading is hereafter named x% Ag/Al_2O_3. For comparison, an Al_2O_3 sample without silver loading was prepared via the same process. In the SO_2 poisoning studies, the samples (2 g) were poisoned in a SO_2-containing gas flow (50 ppm SO_2 + 10% O_2, 1000 mL/min) at 400 °C for 12 h [35], and thus described as x% Ag/Al_2O_3-S.

To study the influence of the nature of the silver species on the sulfur tolerance of Ag/Al_2O_3 catalysts, a 2% Ag/Al_2O_3 sample was synthesized and calcined in air at 900 °C for 3 h, and thereafter named 2%Ag/Al_2O_3-900 [38]. In addition, another 2% Ag/Al_2O_3 sample was synthesized and calcined at 600 °C, with Al_2O_3 pre-calcined at 900 °C as the precursor, and thereafter named 2%Ag/(Al_2O_3-900). The Al_2O_3 sample pre-calcined at 900 °C is named Al_2O_3-900.

The catalytic measurements were carried out in a fixed-bed reactor with inner diameter of 7 mm as reported in our previous works [7,38]. The gas flow (1000 mL/min) consisted of 800 ppm NO, 1714 ppm C_3H_6, 1% H_2, 10% O_2, and 3% H_2O, with N_2 balance. 300 mg catalyst samples (20–40 mesh) were used, thus corresponding to a GHSV of 100 000 h^{-1}. The reactants and products (NO, NO_2, NH_3, N_2O, and C_3H_6) were monitored by a FTIR spectrometer (Nicolet is10). The NO*x* and C_3H_6 conversions and N_2 yield were calculated by the following equations:

$$NOx \quad conversion = \left(1 - \frac{[NO_x]_{out}}{[NO_x]_{in}}\right) \times 100\% \tag{1}$$

$$C_3H_6 \quad conversion = \left(1 - \frac{[C_3H_6]_{out}}{[C_3H_6]_{in}}\right) \times 100\% \tag{2}$$

$$N_2 \quad yield = \left(\frac{[NO_x]_{in} - [NO_x]_{out} - [NH_3]_{out} - 2*[N_2O]_{out}}{[NO_x]_{in}}\right) \times 100\% \tag{3}$$

where NO*x* = NO + NO_2

2.2. Catalyst characterization

BET analysis and X-ray powder diffraction (XRD) measurements were carried out according to our previous works [7,38]. UV–vis measurements were carried out in absorption mode with alumina as reference (Shimadzu, UV3600Plus, Japan). H_2-TPR experiments were carried out on a chemical adsorption instrument (AutoChem II 2920, Micromeritics) equipped with a TCD detector. Before each experiment, the samples (100 mg) were pretreated in 20% O_2/N_2 at 350 °C for 30 min, and subsequently cooled down to 50 °C. The TPR experiments were then performed in 10% H_2/Ar at a rate of 10 °C/min.

TPSR experiments were performed on the Micromeritics AutoChem 2920 apparatus using a MS detector (Cirrus 2, MKS). The poisoned samples (150 mg) were pretreated in Helium at 300 °C for 60 min and then cooled to 50 °C. Then the samples were further heated up (20 °C/min) in a flow of 10%H_2/Ar and 1%H_2/10%O_2/Ar (30 mL/min), respectively.

The amounts of residual sulfates adsorbed on the Ag/Al_2O_3 catalysts after catalytic test were analyzed by ion chromatography. The samples were diluted with ultrapure water to 25 mL and then extracted by sonication for 30 min. The solution was then analyzed using Wayee IC-6200 ion chromatography equipped with a TSKgel Super IC-CR cationic analytical column.

2.3. In situ DRIFTS studies

In situ DRIFTS experiments were performed on a FT-IR spectrometer (Nexus 670, Thermo Nicolet) equipped with an MCT/A detector. The samples were pretreated at 350 °C for 30 min in 10%O_2/N_2 (300 mL/min) and cooled to the desired temperature to collect spectra for reference [7,38]. The concentration of SO_2 in the outlet was monitored by a mass spectrometer (InProcess Instruments, GAM 200).

2.4. DFT calculations

DFT calculations were performed using the Materials Studio (MS) Modeling CASTEP package from Accelrys (Materials Studio 7.0, 2013). Based on previous works [7,11,39,40], the dehydrated (100) and (110) surfaces of γ-Al_2O_3 were modeled. For the Ag ion, AgO units adsorbed on the Al_2O_3 (100) and (110) surfaces were established and relaxed (Fig. S1). For the Ag_n cluster, Ag_3 units adsorbed on the Al_2O_3 (100) and (110) surfaces were established and relaxed (Fig. S2) according to our previous work [11]. Detailed information about the DFT calculations has been provided in the supplementary materials.

The adsorption energies of sulfate (SO_4^{2-}) on the Ag/Al_2O_3 surface were calculated as follows:

$E_{ad} = E_{adsorbate+surface} - (E_{surface} + E_{adsorbate})$,where E_{ad} indicates the adsorption stability of sulfate on the surface of Ag/Al_2O_3.

3. Results

3.1. DeNOx performance and sulfur tolerance

The deNO*x* performance of fresh and poisoned Ag/Al_2O_3 samples was examined in H_2-C_3H_6-SCR (Fig. 1). Except for 1% Ag/Al_2O_3, other fresh samples obtained ~100% NO*x* conversion at ~320 to ~500 °C. Notably, the Ag/Al_2O_3 samples with higher silver loading exhibited better low-temperature deNO*x* performance, especially 4% Ag/Al_2O_3. Furthermore, as the silver loading increased, the light-off temperature of C_3H_6 conversion gradually decreased, consistent with the change in NO*x* conversion (Fig. S3). In our previous works, it was found that increasing the silver loading of Ag/Al_2O_3 usually resulted in a decrease in water tolerance due to the formation of large metallic silver species [7,38]. In the present work, the 4% Ag/Al_2O_3 catalyst showed excellent deNO*x* performance, possibly due to the lower concentration of water vapor (3%), which showed a significant effect on NO*x* reduction in HC-SCR [14]. In addition, the 2% Ag/Al_2O_3-900 and 2% Ag/(Al_2O_3-900) samples exhibited worse water tolerance than that of 2% Ag/Al_2O_3 (not shown), consistent with our previous work [38]. Meanwhile, it was

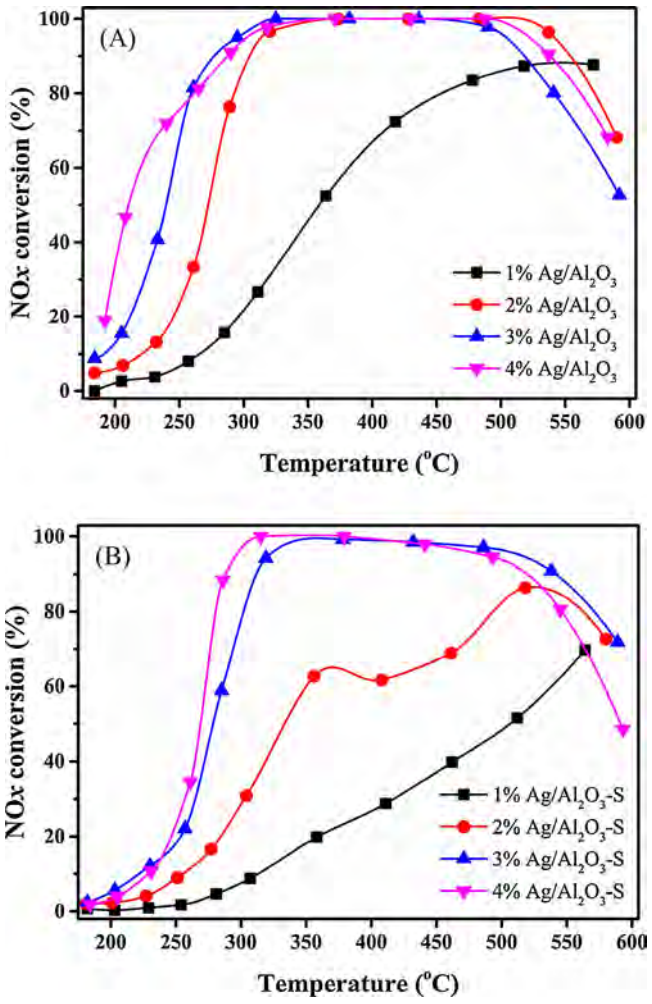

Fig. 1. NO*x* conversions on the Ag/Al_2O_3 (A) and Ag/Al_2O_3-S (B) during the H_2-C_3H_6-SCR. Feed composition: 800 ppm NO, 1714 ppm C_3H_6, 1% H_2, 10% O_2, 3% H_2O, N_2 balance. GHSV: 100 000 h^{-1}.

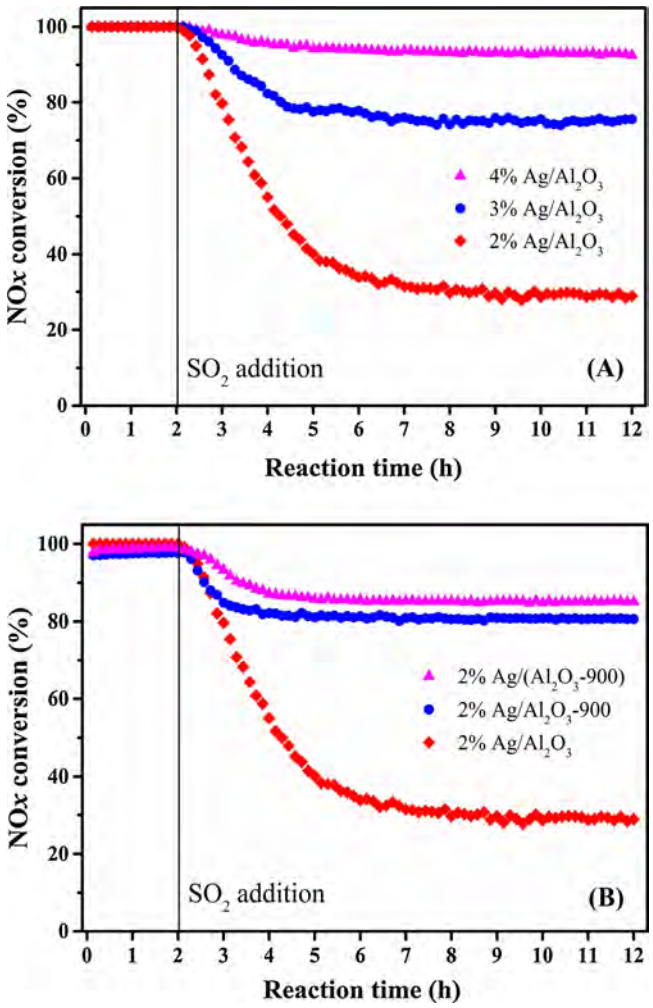

Fig. 2. The effect of SO_2 on the NO*x* conversion over Ag/Al_2O_3 catalysts with different silver loadings (A) and 2%Ag/Al_2O_3 calcined at different temperatures (B) during the H_2-C_3H_6-SCR at 400 °C. Feed composition: 800 ppm NO, 1714 ppm C_3H_6, 1% H_2, 10% O_2, 3% H_2O, 20 ppm SO_2 (when added), N_2 balance. GHSV: 100 000 h^{-1}.

found that the addition of a low amount of H_2 (2000 ppm) also significantly improved the deNO*x* performance of Ag/Al_2O_3 in C_3H_6-SCR [38]. On the poisoned Ag/Al_2O_3 samples, the deNO*x* performance of all samples was suppressed to some extent (Fig. 1B), particularly for those with low silver loadings. For example, the NO*x* conversion decreased from 100% to 61% over 2% Ag/Al_2O_3 after SO_2 poisoning. In contrast, 4% Ag/Al_2O_3-S exhibited excellent deNO*x* performance, achieving > 95% NO*x* conversion in the range of ~300 – ~500 °C.

To further investigate the sulfur tolerance of the Ag/Al_2O_3 catalysts, step-response experiments were performed at 400 °C (Fig. 2). In this case, the 1% Ag/Al_2O_3 sample was not measured due to its poor deNO*x* performance. In the initial stage under SO_2-free conditions, all samples achieved 100% NO*x* conversion. After the introduction of SO_2, the deNO*x* performance of 2% Ag/Al_2O_3 catalyst was severely suppressed and the NO*x* conversion decreased to ~30% after 4 h of SO_2 exposure. Such suppression was also observed over 3% Ag/Al_2O_3, which achieved NO*x* conversion of ~75% after SO_2 exposure. In contrast, 4% Ag/Al_2O_3 exhibited excellent sulfur tolerance and achieved ~93% NO*x* conversion even after 30 h of SO_2 exposure (Fig. S5). Notably, the C_3H_6 conversion exhibited a similar trend as the NO*x* reduction (Fig. S4), revealing the crucial role of C_3H_6 activation in NO*x* reduction.

Meanwhile, the sulfur tolerance of Ag/Al_2O_3 catalysts has been investigated in the H_2-C_3H_6-SCR at a high GHSV of 300 000 h^{-1} at various temperatures (Fig. S6). At 300 °C, the 2% Ag/Al_2O_3 and 3% Ag/Al_2O_3 were almost completely deactivated in the presence of SO_2 with NOx conversions of less than 5%. Under the same reaction conditions, although the NOx conversion of 4% Ag/Al_2O_3 decreased from 80% to 23%, this sample was still the best among these catalysts. At 400 °C, the decrease in NOx conversion for 2% Ag/Al_2O_3 was 69% (from 94% to 25%) after exposure to SO_2, while the corresponding values for 3% Ag/Al_2O_3 and 4% Ag/Al_2O_3 were 25% (from 87% to 62%) and 15% (from 83% to 68%), respectively. At 500 °C, the NOx conversion of 2% Ag/Al_2O_3 and 3% Ag/Al_2O_3 decreased by 41% and 13% after exposure to SO_2, respectively. In contrast, the addition of SO_2 increased the NOx conversion of 4% Ag/Al_2O_3 from 47% to 59% at 500 °C. Similar phenomenon has also been found in the work of Angelidis et al [30], in which this enhancement was attributed to the suppression on direct combustion of reductant. Obviously, the sulfur tolerance of these catalysts enhanced as the reaction temperature increased. From overall view, the Ag/Al_2O_3 samples with higher silver loading exhibited better sulfur tolerance at various temperatures.

Interestingly, the 2% Ag/Al_2O_3-900 and 2% $Ag/(Al_2O_3$-900) samples also exhibited excellent sulfur tolerance in the above step-response experiments, obtaining NO*x* conversion of 80% and 85% in the presence of SO_2, respectively (Fig. 2B). The N_2 yield and C_3H_6 conversion exhibited the same trend as the NO*x* conversion (Fig. S7). Hence, both the silver loading and the state of silver species affected the sulfur tolerance of Ag/Al_2O_3. Considering the difference in sulfur tolerance

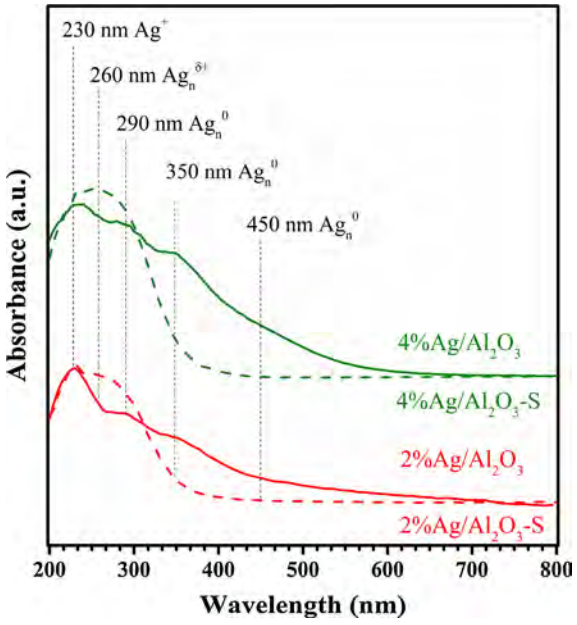

Fig. 3. UV–vis spectra of fresh and SO_2 poisoned 2% Ag/Al_2O_3 and 4% Ag/Al_2O_3.

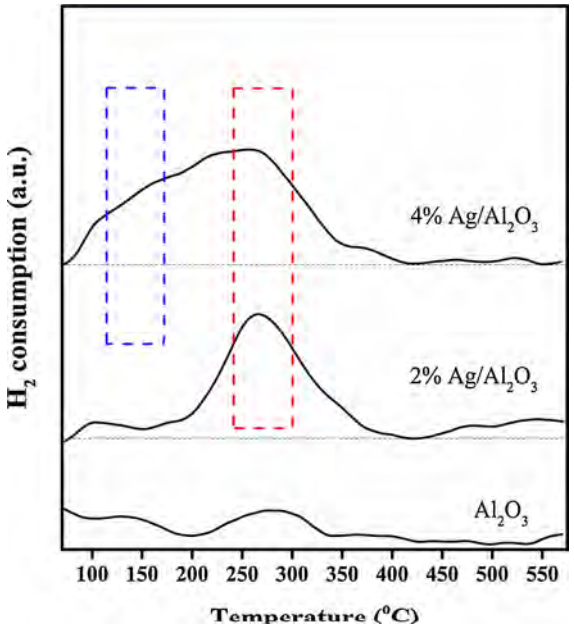

Fig. 4. H_2-TPR profiles of the Al_2O_3 and Ag/Al_2O_3 catalysts.

shown by Ag/Al_2O_3 with 2 and 4 wt% silver loadings, the following investigation focused on these samples.

3.2. Structural properties of Ag/Al_2O_3

BET analysis (Table S1) showed that the specific surface areas of Ag/Al_2O_3 catalysts calcined at 600 °C are similar to that of the pure Al_2O_3 (237 m^2/g). However, calcination at 900 °C caused a decrease in BET surface area of Al_2O_3-900 (163 m^2/g), 2% Ag/Al_2O_3-900 (167 m^2/g), and 2% $Ag/(Al_2O_3$-900) (152 m^2/g). XRD measurements revealed that only the γ-Al_2O_3 phase existed in the Al_2O_3 and Ag/Al_2O_3 catalysts calcined at 600 °C (Fig. S8). In contrast, the δ-Al_2O_3 phase was also detected for the samples calcined at high temperature, together with the presence of γ-Al_2O_3 phase. Therefore, calcination at 900 °C induced the phase transition of γ-Al_2O_3 to δ-Al_2O_3, which further led to the reduction of surface area [38,41]. Furthermore, XRD measurements did not detect any crystal phase of silver species on any of the samples.

Fig. 3 exhibits the UV–vis spectra of fresh and SO_2-poisoned Ag/Al_2O_3 samples. To eliminate interference from the absorption of the support, the spectrum of pure Al_2O_3 was subtracted from the spectra of the Ag/Al_2O_3 samples. For these samples, five adsorption peaks at 230, 260, 290, 350, and 450 nm were observed. According to previous literature [42,43], the peaks located at 230 and 260 nm are commonly attributed to dispersed Ag cations (Ag^+) and oxidized Ag clusters ($Ag_n\delta^+$), respectively. In addition, the peaks at 290 and 350 nm are generally due to small metallic Ag clusters (Ag_n^0), and the broad peak at 450 nm is attributed to metallic Ag clusters with large sizes [43–45].

In order to quantitatively compare different silver species, the spectra of Ag/Al_2O_3 catalysts were fitted and deconvoluted to constituent peaks (Fig. S9 and Table S2) [38,42]. Over the fresh samples, dispersed Ag^+ species were predominant, along with some metallic Ag clusters (Ag_n^0) of different sizes. Notably, the amount of large metallic Ag clusters on 4% Ag/Al_2O_3 (22%) was significantly higher than on 2% Ag/Al_2O_3 (6.6%). The spectrum of Ag/Al_2O_3 calcined at 900 °C is shown in Fig. S9. Compared with 2% Ag/Al_2O_3 (6.6%), there are more metallic Ag clusters with large sizes on 2% Ag/Al_2O_3-900 (35%) and 2% $Ag/(Al_2O_3$-900) (21%). On the poisoned samples, the peaks at 350 and 450 nm almost disappeared, while the intensities of bands with lower wavelengths (260 and 290 nm) increased. This result revealed that SO_2 poisoning induced the transition of metallic silver species to oxidized ones via the following reaction [29]:

$$2Ag + SO_2 + O_2 \rightarrow Ag_2SO_4 \quad (4)$$

H_2-TPR profiles showed that a minuscule H_2 consumption between 250 and 300 °C occurred on the pure Al_2O_3 (Fig. 4), which may be caused by the baseline [46]. Only a strong H_2 consumption peak centered at ~270 °C was observed over for 2% Ag/Al_2O_3. This peak also appeared for 4% Ag/Al_2O_3, accompanied by a low-temperature shoulder at ~100 – ~200 °C. Clearly, both Ag/Al_2O_3 samples contain reducible species (Ag_2O and/or Ag^+), while those on 4% Ag/Al_2O_3 can be reduced at lower temperatures [45–47]. Quantitative data on the H_2 consumption of Ag/Al_2O_3 samples are provided in Table S3. The reduction degree is calculated based on the stoichiometry, such that reduction of 1 mol Ag^+ requires 1/2 mol H_2 [46]. The reduction degrees for 2% Ag/Al_2O_3 and 4% Ag/Al_2O_3 are 64.8% and 46.4%, respectively, indicating that the proportion of non-reducible metallic silver on 4% Ag/Al_2O_3 is higher than on 2% Ag/Al_2O_3. Besides, there are also two H_2 consumption peaks observed on 2% Ag/Al_2O_3-900 and 2% $Ag/(Al_2O_3$-900), the reduction degrees for which are 55.9% and 56.6%, respectively (Fig. S10). Obviously, the proportions of non-reducible metallic silver on these two samples are also higher than on 2% Ag/Al_2O_3. The results of H_2-TPR were consistent with the UV–vis results, further confirming that there were more metallic Ag clusters with large sizes on 4% Ag/Al_2O_3, 2% Ag/Al_2O_3-900, and 2% $Ag/(Al_2O_3$-900) than 2% Ag/Al_2O_3.

To further investigate the adsorption of sulfate species on these samples, TPSR experiments were performed in different atmospheres (Fig. 5). In a reducing atmosphere of 10% H_2/Ar, H_2S (m/z = 34) and SO_2 (m/z = 64) were detected over all poisoned samples (Fig. 5A). On the Al_2O_3-S sample, SO_2 appeared at temperatures above 500 °C, while the signal of H_2S emerged at 550–750 °C. Notably, two peaks of SO_2 centered at ~550 °C and ~650 °C were observed, the latter of which emerged simultaneously with the signal of H_2S. The peak at ~550 °C can be attributed to direct desorption of weakly adsorbed SO_2, and the peak at ~650 °C is assigned to the reduction of sulfates. Over the poisoned Ag/Al_2O_3, it should be noted that H_2S and SO_2 appeared simultaneously at temperatures above 400 °C.

To quantitatively investigate the formation of the above species, all spectra in Fig. 5A were integrated, with the results shown in Table S4. The SO_2 profile of Al_2O_3-S was fitted and deconvoluted into constituent peaks (Fig. S11), which were further integrated. For these samples, the

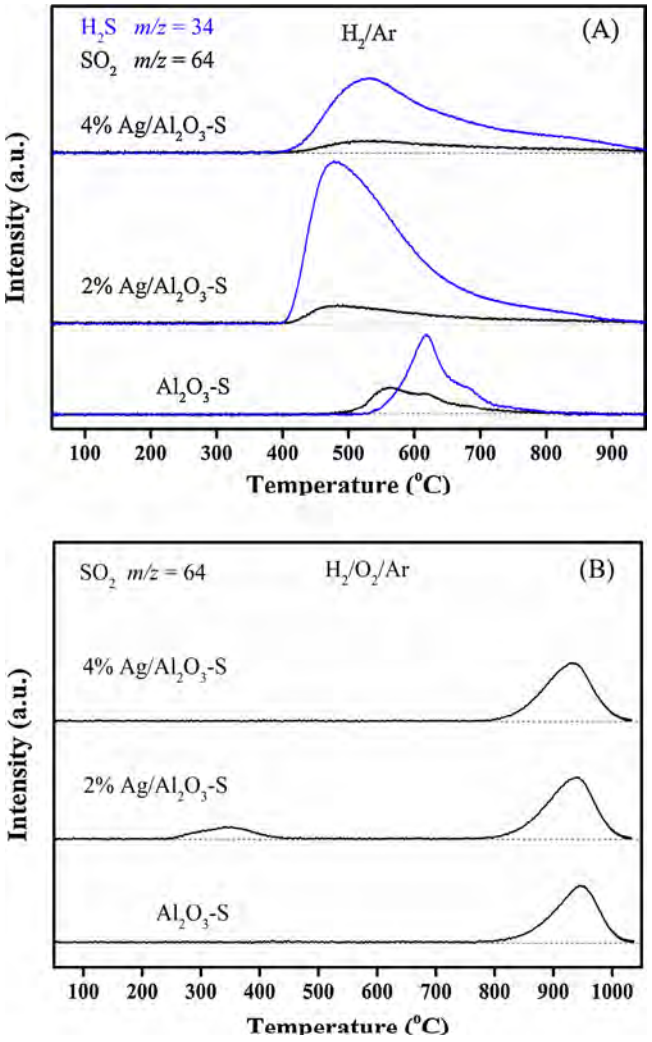

Fig. 5. TPSR spectra of SO_2 poisoned Al_2O_3 and Ag/Al_2O_3 in a flow of 10% H_2/Ar (A) and 1%H_2/10%O_2/Ar (B). Before measurement, the samples were pretreated in a flow of He at 300 °C for 30 min.

amount of desorbed species could be arranged in descending order as follows: 2% Ag/Al_2O_3-S > 4% Ag/Al_2O_3-S > Al_2O_3-S. Notably, the proportion of the desorbed amounts of these species was almost the same over all samples, approximately equal to 0.15: 1 (SO_2/H_2S), revealing the same mechanism for sulfate reduction on all samples.

The TPSR measurements were also performed in a flow of 1%H_2/10%O_2/Ar, which is closer to practical reaction conditions. In this situation, however, only SO_2 (m/z = 64) was detected over all samples, giving a strong peak centered at ~950 °C with almost the same intensity in all cases. The absence of H_2S confirmed that decomposition of sulfates rather than reduction took place during this process. It should be noted that the desorption of sulfur species was much less than that obtained in the reducing atmosphere, revealing that the sulfates showed little decomposition under real reaction conditions. In addition, a weak peak at ~250 – ~400 °C was observed over 2% Ag/Al_2O_3-S, the occurrence of which possibly explained the improvement of deNO*x* performance at 200 ~ 400 °C on this sample (Fig. 1B).

3.3. In situ DRIFTS studies of sulfate species

3.3.1. Sulfate formation and its influence on C_3H_6 oxidation and nitrate formation

In-situ DRIFTS experiment was performed to investigate the adsorption of sulfates on the Ag/Al_2O_3 catalysts during SO_2 poisoning

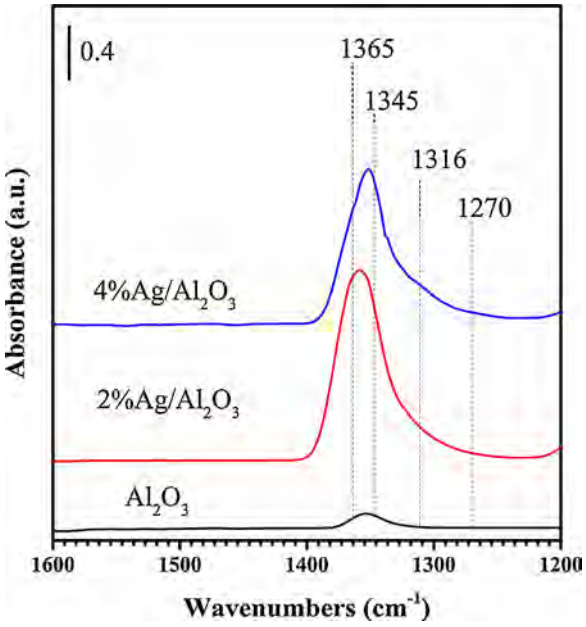

Fig. 6. In situ DRIFTS spectra of adsorbed species over Al_2O_3 and Ag/Al_2O_3 in steady states in a flow of SO_2 + O_2 at 400 °C for 5 h. Feed composition: SO_2 50 ppm, O_2 10%, N_2 balance.

(Fig. 6). In this case, two peaks at 1365 and 1345 cm^{-1} emerged on the pure Al_2O_3, indicating the formation of sulfates adsorbed on the Al sites (Al-sulfates) [28,35]. Over Ag/Al_2O_3 catalysts, the Al-sulfate species were also produced and exhibited much stronger intensity during the above process. Meanwhile, another two bands at 1316 and 1270 cm^{-1} were observed, suggesting the appearance of sulfates adsorbed on the Ag sites (Ag-sulfates) [32,48].

To further compare the adsorption of sulfate species, the above spectra (Fig. 6) were fitted and deconvoluted into constituent peaks (Fig. S12A) [28]. As shown in Fig. S12B, the amounts of sulfates adsorbed on different samples can be arranged as follows: Al_2O_3 (3.6 a.u.) < < 4% Ag/Al_2O_3 (55.8 a.u.) < 2% Ag/Al_2O_3 (71.3 a.u.), which is consistent with the TPSR results. It is generally recognized that SO_2 reacts with O_2 to form ad-SO_4^{2-}, which is further adsorbed on the Ag/Al_2O_3 surface [28,29]. Hence, it could be speculated that the pure Al_2O_3 was inefficient for the oxidation of SO_2, while the existence of Ag significantly enhanced the oxidation of SO_2 to produce ad-SO_4^{2-}, most of which further migrated to the Al sites [28,35]. The smaller amount of sulfate species on 4% Ag/Al_2O_3 may be due to the decrease in acidity of Al_2O_3 with increasing silver loading [49], and/or the decrease in the sites for sulfates adsorption stemmed from the coverage of Al_2O_3 by silver species.

Generally, the activation of hydrocarbons is the initial step of HC-SCR over Ag/Al_2O_3 catalysts [1–4]. Hence, the partial oxidation of C_3H_6 was investigated on the fresh and poisoned Ag/Al_2O_3 samples (Fig. S13). During this process, large amounts of enolic species (1633, 1406, and 1336 cm^{-1}) and acetate (1576 and 1460 cm^{-1}) were produced on the fresh samples, particularly at temperatures below 350 °C [7,50,51]. On 2% Ag/Al_2O_3-S, the formation of enolic species was severely suppressed at temperatures below 350 °C, while acetate was hardly affected except at the temperature of 200 °C. In contrast, a considerable amount of enolic species was yielded on the 4% Ag/Al_2O_3-S at temperatures above 250 °C, while the formation of acetate was slightly enhanced. Furthermore, a weak negative peak at 1365 cm^{-1} attributed to the overlay of sulfates was also observed on the poisoned samples (Fig. S13B and D).

The influence of sulfates on the formation of nitrates was also investigated for these samples (Fig. S14). After exposure to a flow of H_2 + NO + O_2, several strong characteristic peaks (1614, 1582, 1560,

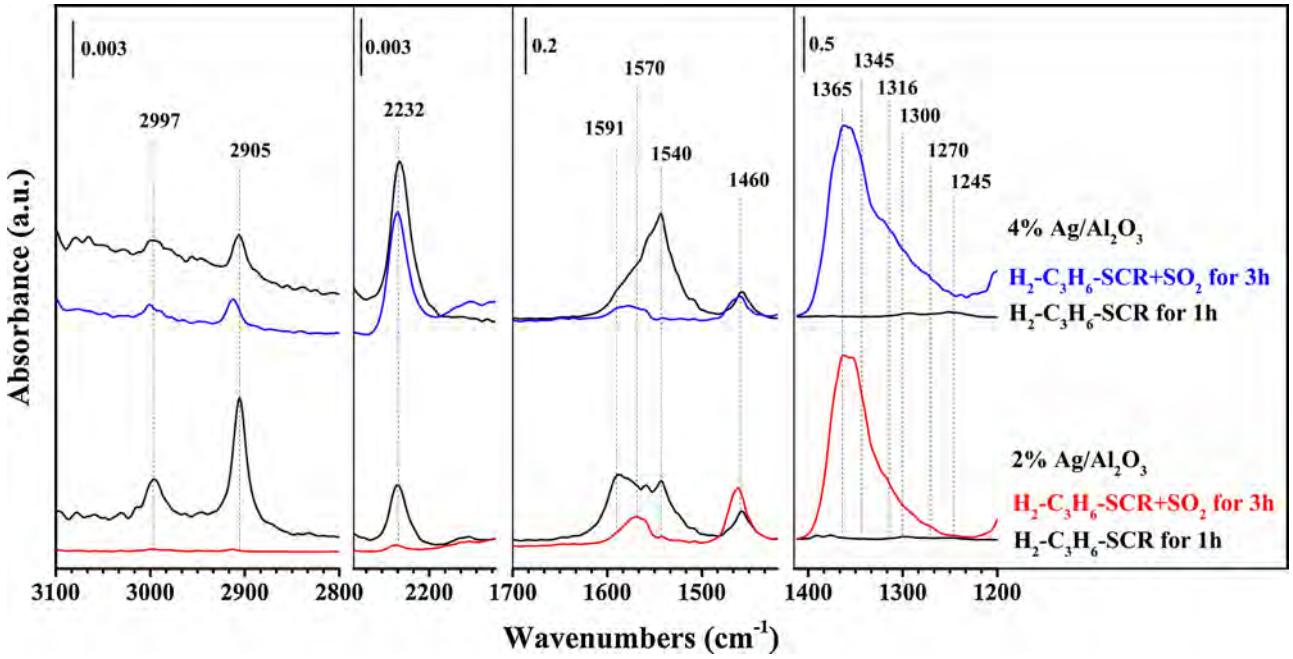

Fig. 7. In situ DRIFTS spectra of adsorbed species over Ag/Al_2O_3 after exposure to a flow of $H_2 + NO + C_3H_6 + SO_2 + O_2$ at 400 °C for 3 h. Before measurement, these samples were pre-exposed to a flow of $H_2 + NO + C_3H_6 + O_2$ at 400 °C for 1 h. Feed composition: 800 ppm NO, 1714 ppm C_3H_6, 1% H_2, 10% O_2, 20 ppm SO_2 (when added), N_2 balance.

1550, 1530, 1300, and 1245 cm^{-1}) were observed on the fresh samples due to monodentate nitrates (1560, 1550, 1530, and 1245 cm^{-1}), bidentate nitrates (1582 and 1300 cm^{-1}), and bridging nitrates (1614 cm^{-1}), respectively [7,38,52]. On the poisoned samples, however, the formation of nitrates was severely suppressed. It is generally recognized that nitrates mainly adsorb on the surface of alumina [1,2], on which sulfates also accumulated seriously during the process of SO_2 poisoning (Fig. 6). Hence, the adsorption of sulfate species reduced the adsorption sites on the Ag/Al_2O_3 available for the formation of nitrates [29,35].

3.3.2. The influence of sulfates on H_2-C_3H_6-SCR over Ag/Al_2O_3

The effect of SO_2 on H_2-C_3H_6-SCR over Ag/Al_2O_3 catalysts was further investigated (Fig. 7). In this case, several intermediates emerged on the Ag/Al_2O_3 surface, including nitrates (1540, 1300, and 1245 cm^{-1}), acetate (1570 and 1460 cm^{-1}), formate (2997, 2905, and 1591 cm^{-1}), and –NCO species (2232 cm^{-1}) [1,2,7]. Among them, the –NCO species is generally recognized as an important intermediate for NOx reduction in HC-SCR [1,2,53,54]. The enolic species was not observed under the current conditions, probably due to its higher reactivity at high temperature (400 °C) [7].

After introducing SO_2 into the gas feed for 3 h, strong peaks due to sulfate species (1365, 1345, 1316, and 1270 cm^{-1}) were observed over both samples. Notably, the intensities of sulfate species were almost the same over these catalysts under the current conditions. Over 2% Ag/Al_2O_3, formate (2997, 2905, and 1591 cm^{-1}) and nitrate (1540 cm^{-1}) were severely suppressed by SO_2 addition, while the intensity of acetate was increased. Notably,–NCO species (2232 cm^{-1}) almost completely disappeared after SO_2 addition, suggesting the severe suppression of the deNO*x* performance. On 4% Ag/Al_2O_3, although the formation the nitrate was serevely inhibited, the –NCO species were hardly affected by SO_2 addition, indicating that this sample exhibited excellent sulfur tolerance, which is consistent with the results in Fig. 2.

The formation of nitrates was severely suppressed by sulfates over both 2%Ag/Al_2O_3 and 4%Ag/Al_2O_3 catalysts, while these samples showed quite different sulfur tolerance in the H_2-C_3H_6-SCR. Therefore, the suppression of the formation of nitrates could not be the key factor in the deactivation of Ag/Al_2O_3. In contrast, sulfates exhibited different influences on the activation of C_3H_6 on these samples (Fig. 7 and Fig. S13). Though formate shows low reactivity toward NO*x* reduction during HC-SCR [7,51], it can serve as a monitor for the activation of C_3H_6. The oxidation of C_3H_6 on 2% Ag/Al_2O_3 was severely suppressed by SO_2 addition, while it was hardly affected on 4% Ag/Al_2O_3. Hence, it was speculated that the inhibition of C_3H_6 activation was more likely to be responsible for the suppression of NO*x* reduction.

3.3.3. The reduction/desorption of sulfates on Ag/Al_2O_3

Although large amounts of sulfates were produced on both samples in the above experiments, they showed markedly different influences on the deNO*x* performance of these catalysts (Fig. 7). To highlight this issue, step-response DRIFTS-MS experiments were performed in different atmospheres (Fig. 8). Specifically, after the formation of sulfates in the above experiment (Fig. 7), the samples were further sequentially exposed to N_2, 1%H_2/N_2, and 1%H_2/10%O_2/N_2. During this process, the dynamic changes of adsorbed species were measured by in situ DRIFTS (Fig. 8A and C), and the SO_2 in the effluent gas was detected by mass spectrometry (m/e = 64) simultaneously (Fig. 8B and D). Furthermore, the corresponding integrated areas of the peaks due to Al-sulfates (1365 and 1345 cm^{-1}) and Ag-sulfates (1316 and 1270 cm^{-1}) were calculated and shown in Fig. 8B and D.

In the first stage of N_2 purging, the amount of Al-sulfates increased slowly, accompanied by a decrease of Ag-sulfates over both samples, indicating that the sulfates adsorbed on Ag sites slowly transferred to Al sites. When switching to 1% H_2/N_2, the sulfate species on 2% Ag/Al_2O_3 decreased very slowly. On 4% Ag/Al_2O_3, in contrast, the Ag-sulfates decreased rapidly in the initial 5 min, accompanied by a slow decrease in the next 25 min (Fig. 8D), and the Al-sulfates rapidly increased in the first minute. Furthermore, a rapid release of SO_2 (m/e = 64) was detected in the effluent gas within the initial 5 min. In the reducing atmosphere, the sulfates adsorbed on Ag sites rapidly transferred to Al sites over 4% Ag/Al_2O_3, while this was hardly observed on 2% Ag/Al_2O_3.

When switching to a flow of 1%H_2/10%O_2/N_2, which is closer to practical reaction conditions, the sulfates on Al sites rapidly migrated to Ag sites, accompanied with release of SO_2 in the gas phase. Notably, such migration was much more remarkable on 4% Ag/Al_2O_3 than 2%

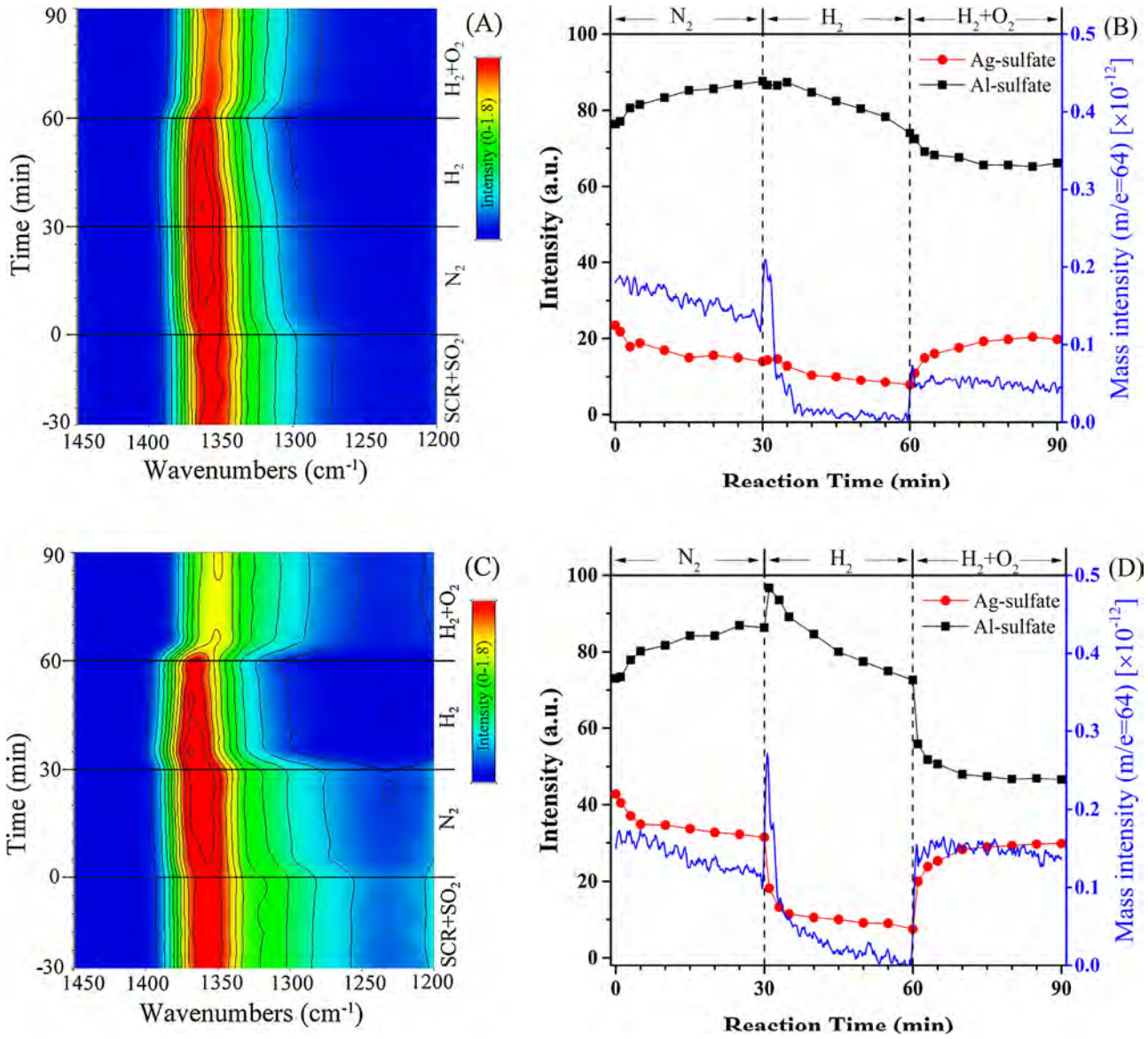

Fig. 8. Dynamic change in the DRIFTS spectra of adsorbed species on 2% Ag/Al_2O_3 (A) and 4% Ag/Al_2O_3 (C) at 400 °C during the gas mixture switching from $H_2/NO/C_3H_6/O_2/SO_2$ (–30 – 0 min) to N_2 (0–30 min), H_2/N_2 (30–60 min), and $H_2/O_2/N_2$ (60–90 min), continuously. Before measurement, the samples were pre-exposed to a flow of $H_2/C_3H_6/NO/SO_2/O_2$ at 400 °C for 3 h. The integrated areas of the peaks (1270 and 1316 cm^{-1}) due to Ag-sulfates and the peaks (1345 and 1365 cm^{-1}) due to Al-sulfates over 2%Ag/Al_2O_3 (B) and 4%Ag/Al_2O_3 (D), together with MS signal of SO_2 (m/e = 64). The feed composition was the same as Fig. 7.

Ag/Al_2O_3. In fact, the amount of SO_2 released in the gas phase from 4% Ag/Al_2O_3 was almost three times that from 2% Ag/Al_2O_3, indicating that more active sites are released for NO*x* reduction. Clearly, the sulfates on 4% Ag/Al_2O_3 were more mobile between Ag sites and Al sites, and were also more easily decomposed and released from the surface. As the sulfur tolerance of 4%Ag/Al_2O_3 was significantly different with the change of reaction temperature, the mobility of sulfate species on this catalyst was further investigated at 300 °C and 500 °C (Fig. S15). In this experiment, the mobility of sulfate species between Ag sites and Al sites was slower at 300 °C if compared with that at 500 °C. This result further confirmed the critical effect of mobility of sulfate species on the sulfur tolerance of Ag/Al_2O_3 catalysts. At 300 °C, notably, the amount of sulfate species adsorbed on the 4% Ag/Al_2O_3 was smaller than that at 400 °C and 500 °C. This may be attributed to the competitive adsorption of oxygenated hydrocarbons at lower temperature [35].

To further investigate the mobility of sulfate species, similar experiments were performed on the 2% Ag/Al_2O_3-900 and 2% $Ag/(Al_2O_3$-900) samples. After exposure to $H_2/SO_2/O_2$ at 400 °C for 3 h, large amounts of sulfate species adsorbed on these samples (Fig. S16). The amounts of Al-sulfate on 2% Ag/Al_2O_3-900 and 2% $Ag/(Al_2O_3$-900) were lower than that on 2% Ag/Al_2O_3, possibly due to the lower BET surface area of the former samples. Afterwards these samples were further sequentially exposed to N_2, 1%H_2/N_2, and 1%H_2/10%O_2/N_2 as described above (Fig. 9 and Fig. S17). On the 2% Ag/Al_2O_3 sample calcined at 600 °C, the sulfates transferred slowly during the above process, accompanied by a low release of SO_2 (Fig. S17). On the 2% Ag/Al_2O_3-900 and 2% $Ag/(Al_2O_3$-900) samples, in contrast, the Ag-sulfates rapidly transferred to Al sites in the reducing atmosphere, and then quickly migrated to Ag sites after switching to a flow of $H_2/O_2/N_2$ (Fig. 9). Obviously, the mobility of sulfates on 2% Ag/Al_2O_3-900 and 2% $Ag/(Al_2O_3$-900) was also greater than that on 2% Ag/Al_2O_3.

3.4. DFT calculations of sulfate adsorption energy

The in-situ DRIFTS experiments showed that the mobility and desorption of sulfates on 4% Ag/Al_2O_3 was much greater than on 2% Ag/

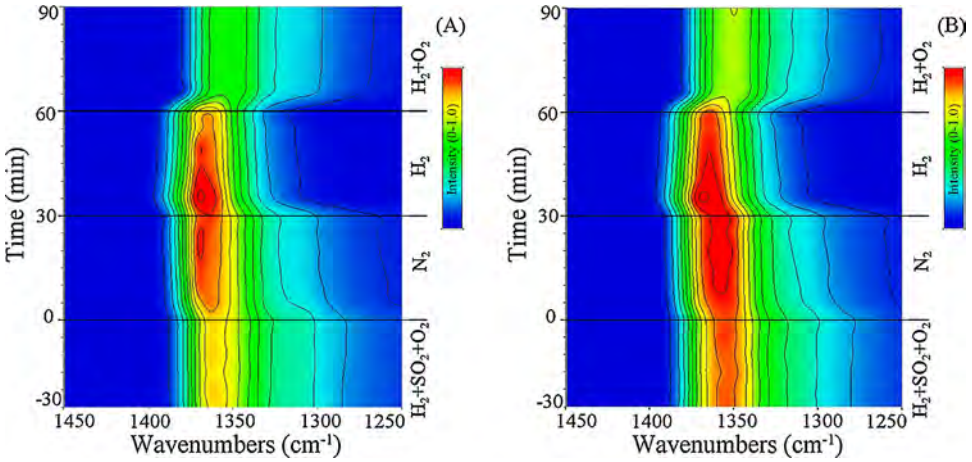

Fig. 9. Dynamic change in the DRIFTS spectra of adsorbed species on the 2%Ag/Al_2O_3-900 (A) and 2%Ag/(Al_2O_3-900) (B) at 400 °C during the gas mixture switching from H_2/SO_2/O_2/N_2 (–30 – 0 min) to N_2 (0–30 min), H_2/N_2 (30–60 min), and H_2/O_2/N_2 (60–90 min), continuously. Before measurement, the samples were pre-exposed to a flow of $H_2 + SO_2 + O_2$ at 400 °C for 3 h (Fig. S16).

Al_2O_3. Hence, the adsorption energies of sulfates on the surface of Ag/Al_2O_3 were calculated. UV–vis and H_2-TPR measurements confirmed that dispersed Ag^+ cations were predominant on 2% Ag/Al_2O_3, while more Ag clusters were present on 4% Ag/Al_2O_3. As a result, Ag_1 cations and Ag_3 clusters supported on the Al_2O_3 (110) and (100) surface were established and relaxed, which are hereafter described as Ag_1-Al_2O_3 and Ag_3-Al_2O_3 (Fig. S1 and S2), corresponding to 2% Ag/Al_2O_3 and 4% Ag/Al_2O_3, respectively [11,55]. The structures of sulfates adsorbed on the Ag and Al sites of the above models were established and relaxed (Fig. S18 and S19).

The DFT calculations showed that the adsorption energies of sulfates are negative, indicating a strong affinity between the sulfates and the catalyst surface (Table 1). Over the Ag_1-Al_2O_3 sample, the adsorption energies of sulfates adsorbed on the Ag_1 sites of (110) and (100) surfaces were 12% and 28% less negative than those on the corresponding Al sites, respectively. Similarly, the adsorption energies of sulfates on the Ag_3 clusters of (110) and (100) surfaces were significantly less negative than those on the Al sites over the Ag_3-Al_2O_3 sample. On both samples, the adsorption energies of sulfates adsorbed on the Ag sites were less negative than those on the Al sites, indicating that desorption of sulfates from the Ag sites was easier than that from Al sites. Furthermore, the adsorption energy of sulfates on the Ag_3 clusters was less negative than for those adsorbed on the Ag_1 cation, especially on the (100) surface. This result revealed that desorption of sulfates from the Ag_3 clusters was more efficient than that from Ag_1 cations.

The above results show that the adsorption energies of sulfates can be arranged as follows: $|Ag_3| < |Ag_1| < |Al|$ sites, consistent with Doronkin's work [56], in which the SO_2 resistance of Ag/Al_2O_3 in H_2-NH_3-SCR was investigated. In that work, the authors calculated the adsorption energies of SO*x* species on the surfaces of bulk silver, Al_2O_3, and a single-atom Ag site, and found that SO*x* species bind weaklier to the bulk silver surface than to Al_2O_3 and the single-atom Ag site. Notably, the adsorption energy of SO_4^{2-} on the Ag (111) surface (-2.65 eV) in that work is consistent with the adsorption energy of sulfates on the Ag_3 clusters of the (110) surface (-2.43 eV). Therefore, the calculations of the adsorption energies of sulfates in the present work are believed to be reliable.

Table 1
DFT-calculated adsorption energies of sulfates on different sites of Ag/Al_2O_3.

Site	adsorption energy (eV)	
	Ag/Al_2O_3(110)	Ag/Al_2O_3(100)
(Ag_1-Al_2O_3)-Al	–3.04	–3.58
(Ag_1-Al_2O_3)-Ag_1	–2.69 (–12%)	–2.56 (–28%)
(Ag_3-Al_2O_3)-Al	–2.77	–2.80
(Ag_3-Al_2O_3)-Ag_3	–2.43 (–12%)	–1.63 (–42%)

4. Discussion

It is generally recognized that the HC-SCR reaction starts with the activation of HCs to yield reactive oxygenated hydrocarbons such as enolic species and acetates [1,2]. As for H_2-C_3H_6-SCR over Ag/Al_2O_3 catalyst, the activation of reductant involves the activation of C—C bonds and/or C–H bonds, the occurrence of which require O species adsorbed on silver species and/or the electrons provided by silver species [42]. Hence, the activation of C_3H_6 primarily occurs at the Ag sites of the Ag/Al_2O_3 catalyst. The above reactive oxygenated hydrocarbons further react with NO + O_2 and/or nitrate (adsorbed on the Al sites adjacent to the Ag sites) to produce the –NCO species, which is also anchored at the Ag sites or the interface between Ag sites and Al_2O_3 support [53,54,57,58]. Then the –NCO species reacts either directly with NO + O_2 and/or nitrate to produce N_2 or with water vapor to produce NH_3, which further reacts with NO + O_2 and/or nitrate to produce N_2 [53,54]. Clearly, the Ag sites and the interface between Ag sites and Al sites (denoted as Ag-O-Al interface) is critical for NO*x* reduction in HC-SCR over Ag/Al_2O_3 [53,54,57].

On Ag/Al_2O_3 catalysts, the formation of sulfates starts with the oxidation of SO_2 on Ag sites, followed by further migration to Al sites [28,35]. UV–vis analysis revealed that adsorption of sulfates induced the transition of metallic silver to oxidized silver on Ag/Al_2O_3. In a reducing atmosphere, H_2 facilitated the reduction of oxidized silver species, providing a driving force for the migration of sulfates from Ag sites to Al sites and the desorption of sulfates to yield SO_2 (Fig. 8). The sulfates adsorbed on the Al sites were further reduced to yield H_2S and SO_2 (Fig. 5A). In a similar reducing atmosphere, Shimizu et al. [32] also observed a migration of sulfates from Ag sites to Al sites and desorption of SO_2 during H_2-C_3H_8-SCR over Ag/Al_2O_3. In that case, it was proposed that H_2 cleaned off the sulfates adsorbed on the Ag sites, and thus enhanced the sulfur tolerance of Ag/Al_2O_3. In the atmosphere of 1%H_2/10%O_2/N_2, which is closer to practical reaction conditions, however, the sulfates cannot actually be reduced to H_2S and SO_2 (Fig. 5B). In contrast, the Al-sulfates rapidly migrated to the Ag sites where they were further decomposed to produce SO_2. Hence, a cyclic pathway of sulfate formation and desorption between Ag sites and Al sites was observed on the surface of Ag/Al_2O_3.

DFT calculations revealed that the adsorption energies of sulfates on different sites of Ag/Al_2O_3 can be arranged as follows: $|Ag_3| < |Ag_1| < |Al|$ sites. Therefore, desorption of sulfates from Ag_3 clusters was more efficient than from Ag_1 cations, while the desorption of sulfates from Al sites was inefficient. UV–vis analysis showed that there were more metallic Ag clusters with large sizes present on 4% Ag/Al_2O_3 compared to 2% Ag/Al_2O_3. Hence, it is reasonable that the desorption of sulfates on 4% Ag/Al_2O_3 surface was more rapid than that on 2% Ag/Al_2O_3. The H_2-TPR experiment revealed that the silver species

on 4% Ag/Al_2O_3 were more easily reduced at lower temperatures than those on 2% Ag/Al_2O_3. Hence, the migration of sulfates from Ag sites to Al sites in a reducing atmosphere on 4% Ag/Al_2O_3 was also more rapid than that on 2% Ag/Al_2O_3. In the flow of 1%H_2/10%O_2/N_2, the rapid migration of sulfates from Al sites to Ag sites on 4% Ag/Al_2O_3 could be attributed to the great difference in adsorption energies of sulfates on Ag clusters and Al_2O_3 surface. In contrast, the Ag^+ showed strong affinity for sulfate species, resulting in the blockage by sulfates on the 2% Ag/Al_2O_3.

To further investigate the mobility of sulfate species, 2% Ag/Al_2O_3 catalysts were synthesized and calcined at higher temperature. Calcination at 900 °C induced the phase transition of γ-Al_2O_3 to δ-Al_2O_3, which further led to the reduction of surface area for 2% Ag/Al_2O_3-900 and 2% Ag/(Al_2O_3-900). Besides, the formation of δ-Al_2O_3 further induced the aggregation of dispersed Ag^+ cations to produce large Ag clusters. Hence, the amounts of large Ag clusters on these two samples were significantly greater than that on 2% Ag/Al_2O_3 calcined at 600 °C (Table S2). The DRIFTS-MS experiment shows that the mobility of sulfate species on the samples calcined at high temperature was greater than that on 2% Ag/Al_2O_3 (Fig. 9), further confirming that the mobility of sulfur species was closely related to the state of silver species.

The deNO*x* performance of 2%Ag/Al_2O_3 was severely suppressed after exposure to SO_2 for 3 h (Fig. 2), while the 4%Ag/Al_2O_3 catalyst maintained high NO*x* conversion even after 30 h of SO_2 exposure (Fig. S5). The results of ion chromatography show that after exposure to 20 ppm SO_2 for 10 h (Fig. 2), the amount of SO_2 deposited on the 2%Ag/Al_2O_3, 3%Ag/Al_2O_3, and 4%Ag/Al_2O_3 were 7.79×10^{-5} mol/g, 9.50×10^{-5} mol/g, and 8.96×10^{-5} mol/g, respectively. This indicates that the amounts of sulfates adsorbed on these catalysts were approximately equal, consistent with the DRIFTS results (Fig. 7). On the 4%Ag/Al_2O_3, the amount of sulfate species adsorbed at 300 °C was even smaller than those at 400 °C and 500 °C (Fig. S15), while this sample exhibited poorer sulfur tolerance at 300 °C. Considering the above results, the amount of sulfate species adsorbed on the surface cannot reasonably explain the different sulfur tolerance of these Ag/Al_2O_3 catalysts. Hence, there are other factors governing the sulfur tolerance of Ag/Al_2O_3 catalysts.

As mentioned above, the H_2-C_3H_6-SCR reaction starts with the activation of C_3H_6 to yield reactive oxygenated hydrocarbons such as enolic species and acetates, which primarily occurs at the Ag sites and the Ag-O-Al interface [7,42]. The adsorption of sulfate species on the Ag/Al_2O_3 catalysts induces the formation of Ag-sulfates and/or Ag_2SO_4 species. In particular, Ag^+ cations show strong affinity for sulfate species, resulting in the blockage of sulfates on the 2%Ag/Al_2O_3. The formation of Ag-sulfates and/or Ag_2SO_4 species may affect the electron-donating ability of silver species, and thus inhibits the activation of C_3H_6 to produce enolic species on the 2%Ag/Al_2O_3 (Fig. S13). Furthermore, the strong adsorption of sulfate species may hinder the reaction between C_3H_6 and O species on the Ag sites due to a strong steric effect. Afterward, these effects induced by sulfates may further hinder the reaction between enolic species and NO + O_2 (and/or nitrate) to produce -NCO species, finally resulting in the suppression on the deNOx performance of 2% Ag/Al_2O_3 catalyst (Fig. 7). Besides, the formation of nitrates was severely suppressed due to competitive adsorption of sulfates on Al_2O_3 surface (Fig. S14). However, the adsorption of nitrates on the Al sites far from Ag sites showed little effect on the reduction of NO*x* as the reaction primarily occurred at the Ag sites and Ag-O-Al interface [53,54,57,58].

On the Ag/Al_2O_3 catalysts with large amounts of Ag clusters (4% Ag/Al_2O_3, 2% Ag/Al_2O_3-900, and 2% Ag/(Al_2O_3-900)), the sulfates were more mobile between Ag sites and Al sites, and were also more easily decomposed and released from the surface. The rapid mobility of sulfate species at the Ag-O-Al interface provided an opportunity for the reaction between C_3H_6, NO, and O species at the Ag sites. Hence, the above suppression induced by sulfates was weakened due to the rapid mobility of sulfate species at the Ag-O-Al interface. Over these samples, as a result, more active sites were available for the formation of enolic species, acetates, and -NCO species, which have been observed in Fig. S13 and Fig. 7. Hence, the rapid mobility of sulfate species showed an important effect on the sulfur tolerance of Ag/Al_2O_3 catalysts. At 300 °C, the slow mobility of sulfates induced a poor sulfur tolerance of 4% Ag/Al_2O_3, which in turn confirmed the critical effect of mobility of sulfates on the sulfur tolerance of Ag/Al_2O_3. As mentioned above, the sulfate species transferred rapidly between Ag clusters and Al_2O_3 surface due to the weak affinity of Ag clusters for sulfates. Therefore, increasing the number of Ag clusters on the Ag/Al_2O_3 catalysts helps to enhance the mobility of sulfates at the Ag-O-Al interface, and thus improved the sulfur tolerance of these catalysts.

5. Conclusion

The sulfur tolerance of Ag/Al_2O_3 in the H_2-C_3H_6-SCR is governed by the mobility of sulfate species, which is closely related to the state of silver species. Highly dispersed Ag^+ predominates on 2% Ag/Al_2O_3, while more metallic Ag clusters with large sizes are present on 4% Ag/Al_2O_3. High temperature calcination promoted the transformation of γ-Al_2O_3 into δ-Al_2O_3, which induced the aggregation of dispersed Ag^+ cations to produce large Ag clusters on 2% Ag/Al_2O_3-900 and 2% Ag/(Al_2O_3-900). DFT calculations reveals that Ag_1 cations show strong affinity for sulfate species, resulting in blockage by sulfates at the Ag-O-Al interface on 2% Ag/Al_2O_3. Such blocking by sulfates suppressed the activation of C_3H_6 and the formation of -NCO species as well as its further transformation, thus severely inhibiting the deNO*x* performance of 2% Ag/Al_2O_3. In contrast, the weak affinity of Ag clusters for sulfates led the rapid migration of sulfates between Ag clusters and Al sites. The rapid migration of sulfates at the Ag-O-Al interface had little effect on the formation of enolic species and -NCO species, and thus contributed to the excellent sulfur tolerance observed for 4% Ag/Al_2O_3, 2% Ag/Al_2O_3-900, and 2% Ag/(Al_2O_3-900). Hence, developing Ag/Al_2O_3 catalysts with more Ag clusters is crucial to improve the sulfur tolerance of HC-SCR.

Acknowledgments

This work was supported by the National Key R&D Program of China (2017YFC0211105 and 2017YFC0211101), the National Natural Science Foundation of China (21673277 and 21637005), the K.C.Wong Education Foundation, and the Youth Innovation Promotion Association, CAS (2017064).

Appendix A. Supplementary data

Supplementary material related to this article can be found, in the online version, at doi:https://doi.org/10.1016/j.apcatb.2018.11.050.

References

[1] R. Burch, J.P. Breen, F.C. Meunier, A review of the selective reduction of NOx with hydrocarbons under lean-burn conditions with non-zeolitic oxide and platinum group metal catalysts, Appl. Catal. B: Environ. 39 (2002) 283–303.
[2] H. He, Y.B. Yu, Selective catalytic reduction of NOx over Ag/Al_2O_3 catalyst: from reaction mechanism to diesel engine test, Catal. Today 100 (2005) 37–47.
[3] K. Shimizu, K. Sawabe, A. Satsuma, Unique catalytic features of Ag nanoclusters for selective NOx reduction and green chemical reactions, Catal. Sci. Technol. 1 (2011) 331–341.
[4] Z.M. Liu, S.I. Woo, Recent advances in catalytic DeNOx science and technology, Catal. Rev. 48 (2006) 43–89.
[5] M. Barreau, M.L. Tarot, D. Duprez, X. Courtois, F. Can, Remarkable enhancement of the selective catalytic reduction of NO at low temperature by collaborative effect of ethanol and NH_3 over silver supported catalyst, Appl. Catal. B: Environ. 220 (2018) 19–30.
[6] F. Gunnarsson, J.A. Pihl, T.J. Toops, M. Skoglundh, H. Harelind, Lean NOx reduction over Ag/alumina catalysts via ethanol-SCR using ethanol/gasoline blends, Appl. Catal. B: Environ. 202 (2017) 42–50.
[7] G.Y. Xu, J.Z. Ma, G.Z. He, Y.B. Yu, H. He, An alumina-supported silver catalyst with

high water tolerance for H_2 assisted C_3H_6-SCR of NOx, Appl. Catal. B: Environ. 207 (2017) 60–71.
[8] M. Mannikko, X.T. Wang, M. Skoglundh, H. Harelind, Silver/alumina for methanol-assisted lean NOx reduction On the influence of silver species and hydrogen formation, Appl. Catal. B: Environ. 180 (2016) 291–300.
[9] P.M. More, D.L. Nguyen, M.K. Dongare, S.B. Umbarkar, N. Nuns, J.S. Girardon, C. Dujardin, C. Lancelot, A.S. Mamede, P. Granger, Rational preparation of Ag and Au bimetallic catalysts for the hydrocarbon-SCR of NOx: Sequential deposition vs. coprecipitation method, Appl. Catal. B: Environ. 162 (2015) 11–20.
[10] P.M. More, D.L. Nguyen, P. Granger, C. Dujardin, M.K. Dongare, S.B. Umbarkar, Activation by pretreatment of Ag-Au/Al_2O_3 bimetallic catalyst to improve low temperature HC-SCR of NOx for lean burn engine exhaust, Appl. Catal. B: Environ. 174 (2015) 145–156.
[11] H. Deng, Y.B. Yu, F.D. Liu, J.Z. Ma, Y. Zhang, H. He, Nature of Ag species on Ag/gamma-Al_2O_3: a combined experimental and theoretical study, ACS Catal. 4 (2014) 2776–2784.
[12] T. Chaieb, L. Delannoy, G. Costentin, C. Louis, S. Casale, R.L. Chantry, Z.Y. Li, C. Thomas, Insights into the influence of the Ag loading on Al_2O_3 in the H_2-assisted C_3H_6-SCR of NOx, Appl. Catal. B: Environ. 156 (2014) 192–201.
[13] T. Chaieb, L. Delannoy, C. Louis, C. Thomas, On the origin of the optimum loading of Ag on Al_2O_3 in the C_3H_6-SCR of NOx, Appl. Catal. B: Environ. 142 (2013) 780–784.
[14] G.Y. Xu, Y.B. Yu, H. He, A Low-Temperature Route Triggered by Water Vapor during the Ethanol-SCR of NOx over Ag/Al_2O_3, ACS Catal. 8 (2018) 2699–2708.
[15] S. Satokawa, Enhancing the NO/C_3H_8/O_2 reaction by using H_2 over Ag/Al_2O_3 catalysts under lean-exhaust conditions, Chem. Lett. (2000) 294–295.
[16] S. Satokawa, J. Shibata, K. Shimizu, S. Atsushi, T. Hattori, Promotion effect of H_2 on the low temperature activity of the selective reduction of NO by light hydrocarbons over Ag/Al_2O_3, Appl. Catal. B: Environ. 42 (2003) 179–186.
[17] K. Shimizu, J. Shibata, A. Satsuma, Kinetic and in situ infrared studies on SCR of NO with propane by silver-alumina catalyst: role of H_2 on O_2 activation and retardation of nitrate poisoning, J. Catal. 239 (2006) 402–409.
[18] P.S. Kim, M.K. Kim, B.K. Cho, I.S. Nam, S.H. Oh, Effect of H_2on deNOx performance of HC-SCR over Ag/Al_2O_3: Morphological, chemical, and kinetic changes, J. Catal. 301 (2013) 65–76.
[19] J.P. Breen, R. Burch, C. Hardacre, C.J. Hill, C. Rioche, A fast transient kinetic study of the effect of H_2 on the selective catalytic reduction of NOx with octane using isotopically labelled (NO)-N-15, J. Catal. 246 (2007) 1–9.
[20] C. Thomas, On an additional promoting role of hydrogen in the H_2-assisted C_3H_6-SCR of NOx on Ag/Al_2O_3: A lowering of the temperature of formation-decomposition of the organo-NOx intermediates? Appl. Catal. B: Environ. 162 (2015) 454–462.
[21] L. Strom, P.A. Carlsson, M. Skoglundh, H. Harelind, Hydrogen-assisted SCR of NOx over alumina-supported silver and indium catalysts using C_2-hydrocarbons and oxygenates, Appl. Catal. B: Environ. 181 (2016) 403–412.
[22] Y.B. Yu, Y. Li, X.L. Zhang, H. Deng, H. He, Y.Y. Li, Promotion effect of H_2 on ethanol oxidation and NO reduction with ethanol over Ag/Al_2O_3 catalyst, Environ. Sci. Technol. 49 (2015) 481–488.
[23] F. Gunnarsson, M.Z. Granlund, M. Englund, J. Dawody, L.J. Pettersson, H. Harelind, Combining HC-SCR over Ag/Al_2O_3 and hydrogen generation over Rh/CeO_2-ZrO_2 using biofuels: an integrated system approach for real applications, Appl. Catal. B: Environ. 162 (2015) 583–592.
[24] M.M. Azis, H. Harelind, D. Creaser, On the role of H_2 to modify surface NOx species over Ag-Al_2O_3 as lean NOx reduction catalyst: TPD and DRIFTS studies, Catal. Sci. Technol. 5 (2015) 296–309.
[25] P.S. Hammershoi, A.D. Jensen, T.V.W. Janssens, Impact of SO_2-poisoning over the lifetime of a Cu-CHA catalyst for NH_3-SCR, Appl. Catal. B: Environ. 238 (2018) 104–110.
[26] P.S. Hammershoi, Y. Jangjou, W.S. Epling, A.D. Jensen, T.V.W. Janssens, Reversible and irreversible deactivation of Cu-CHA NH_3-SCR catalysts by SO_2 and SO_3, Appl. Catal. B: Environ. 226 (2018) 38–45.
[27] K. Wijayanti, K.P. Xie, A. Kumar, K. Kamasamudram, L. Olsson, Effect of gas compositions on SO_2 poisoning over Cu/SSZ-13 used for NH_3-SCR, Appl. Catal. B: Environ. 219 (2017) 142–154.
[28] K. Shimizu, T. Higashimata, M. Tsuzuki, A. Satsuma, Effect of hydrogen addition on SO_2 tolerance of silver-alumina for SCR of NO with propane, J. Catal. 239 (2006) 117–124.
[29] F.C. Meunier, J.R.H. Ross, Effect of ex situ treatments with SO_2 on the activity of a low loading silver-alumina catalyst for the selective reduction of NO and NO_2 by propene, Appl. Catal. B: Environ. 24 (2000) 23–32.
[30] T.N. Angelidis, S. Christoforou, A. Bongiovanni, N. Kruse, On the promotion by SO_2 of the SCR process over Ag/Al_2O_3: influence of SO_2 concentration with C_3H_6 versus C_3H_8 as reductant, Appl. Catal. B: Environ. 39 (2002) 197–204.
[31] P.W. Park, C.L. Boyer, Effect of SO_2 on the activity of Ag/gamma-Al_2O_3 catalysts for NOx reduction in lean conditions, Appl. Catal. B: Environ. 59 (2005) 27–34.
[32] K.I. Shimizu, M. Tsuzuki, A. Satsuma, Effects of hydrogen and oxygenated hydrocarbons on the activity and SO_2-tolerance of Ag/Al_2O_3 for selective reduction of NO, Appl. Catal. B: Environ. 71 (2007) 80–84.
[33] P.M. More, N. Jagtap, A.B. Kulal, M.K. Dongare, S.B. Umbarkar, Magnesia doped Ag/Al_2O_3 - Sulfur tolerant catalyst for low temperature HC-SCR of NOx, Appl. Catal. B: Environ. 144 (2014) 408–415.
[34] V. Houel, P. Millington, S. Pollington, S. Poulston, R.R. Rajaram, A. Tsolakis, Chemical deactivation of Ag/Al_2O_3 by sulphur for the selective reduction of NOx using hydrocarbons, Catal. Today 114 (2006) 334–339.
[35] S.X. Xie, J. Wang, H. He, Poisoning effect of sulphate on the selective catalytic reduction of NOx by C_3H_6 over Ag-Pd/Al_2O_3, J Mol. Catal. A: Chem 266 (2007) 166–172.
[36] J.H. Li, Y.Q. Zhu, R. Ke, J.M. Hao, Improvement of catalytic activity and sulfur-resistance of Ag/TiO_2-Al_2O_3 for NO reduction with propene under lean burn conditions, Appl. Catal. B: Environ. 80 (2008) 202–213.
[37] Y. Shi, H. Pan, Y.T. Zhang, W. Li, Promotion of MgO addition on SO_2 tolerance of Ag/Al_2O_3 for selective catalytic reduction of NOx with methane at low temperature, Catal. Commun. 9 (2008) 796–800.
[38] G.Y. Xu, Y.B. Yu, H. He, Silver Valence State Determines the Water Tolerance of Ag/Al_2O_3 for the H_2-C_3H_6-SCR of NOx, J. Phys. Chem. C 122 (2018) 670–680.
[39] M. Digne, P. Sautet, P. Raybaud, P. Euzen, H. Toulhoat, Hydroxyl groups on gamma-alumina surfaces: a DFT study, J. Catal. 211 (2002) 1–5.
[40] M. Digne, P. Sautet, P. Raybaud, P. Euzen, H. Toulhoat, Use of DFT to achieve a rational understanding of acid-basic properties of gamma-alumina surfaces, J. Catal. 226 (2004) 54–68.
[41] D.Y. Yoon, J.H. Park, H.C. Kang, P.S. Kim, I.S. Nam, G.K. Yeo, J.K. Kil, M.S. Cha, DeNOx performance of Ag/Al_2O_3 catalyst by n-dodecane: Effect of calcination temperature, Appl. Catal. B: Environ. 101 (2011) 275–282.
[42] Y. Yan, Y.B. Yu, H. He, J.J. Zhao, Intimate contact of enolic species with silver sites benefits the SCR of NOx by ethanol over Ag/Al_2O_3, J. Catal. 293 (2012) 13–26.
[43] J. Shibata, K. Shimizu, Y. Takada, A. Shichia, H. Yoshida, S. Satokawa, A. Satsuma, T. Hattori, Structure of active Ag clusters in Ag zeolites for SCR of NO by propane in the presence of hydrogen, J. Catal. 227 (2004) 367–374.
[44] J. Shibata, Y. Takada, A. Shichi, S. Satokawa, A. Satsuma, T. Hattori, Ag cluster as active species for SCR of NO by propane in the presence of hydrogen over Ag-MFI, J. Catal. 222 (2004) 368–376.
[45] K.A. Bethke, H.H. Kung, Supported Ag catalysts for the lean reduction of NO with C_3H_6, J. Catal. 172 (1997) 93–102.
[46] M. Richter, U. Bentrup, R. Eckelt, M. Schneider, M.M. Pohl, R. Fricke, The effect of hydrogen on the selective catalytic reduction of NO in excess oxygen over Ag/Al_2O_3, Appl. Catal. B: Environ. 51 (2004) 261–274.
[47] T. Furusawa, K. Seshan, J.A. Lercher, L. Lefferts, K. Aika, Selective reduction of NO to N_2 in the presence of oxygen over supported silver catalysts, Appl. Catal. B: Environ. 37 (2002) 205–216.
[48] Q. Wu, H.W. Gao, H. He, Conformational analysis of sulfate species on Ag/Al_2O_3 by means of theoretical and experimental vibration spectra, J. Phys. Chem. B 110 (2006) 8320–8324.
[49] Z.M. Wang, M. Yamaguchi, I. Goto, M. Kumagai, Characterization of Ag/Al2O_3 de-NOx catalysts by probing surface acidity and basicity of the supporting substrate, Phys. Chem. Chem. Phys. 2 (2000) 3007–3015.
[50] M.K. Kim, P.S. Kim, J.H. Baik, I.S. Nam, B.K. Cho, S.H. Oh, DeNOx performance of Ag/Al_2O_3 catalyst using simulated diesel fuel-ethanol mixture as reductant, Appl. Catal. B: Environ. 105 (2011) 1–14.
[51] Y.B. Yu, X.P. Song, H. He, Remarkable influence of reductant structure on the activity of alumina-supported silver catalyst for the selective catalytic reduction of NOx, J. Catal. 271 (2010) 343–350.
[52] Y.B. Yu, H. He, Q.C. Feng, H.W. Gao, X. Yang, Mechanism of the selective catalytic reduction of NOx by C_2H_5OH over Ag/Al_2O_3, Appl. Catal. B: Environ. 49 (2004) 159–171.
[53] N. Bion, J. Saussey, M. Haneda, M. Daturi, Study by in situ FTIR spectroscopy of the SCR of NO, by ethanol on Ag/Al_2O_3 - Evidence of the role of isocyanate species, J. Catal. 217 (2003) 47–58.
[54] S. Tamm, H.H. Ingelsten, A.E.C. Palmqvist, On the different roles of isocyanate and cyanide species in propene-SCR over silver/alumina, J. Catal. 255 (2008) 304–312.
[55] H. Deng, Y.B. Yu, H. He, Discerning the Role of Ag-O-Al Entities on Ag/gamma-Al_2O_3Surface in NOx Selective Reduction by Ethanol, J Phys. Chem. C 119 (2015) 3132–3142.
[56] D.E. Doronkin, T.S. Khan, T. Bligaard, S. Fogel, P. Gabrielsson, S. Dahl, Sulfur poisoning and regeneration of the Ag/gamma-Al_2O_3 catalyst for H_2-assisted SCR of NOx by ammonia, Appl. Catal. B: Environ. 117 (2012) 49–58.
[57] F. Thibault-Starzyk, E. Seguin, S. Thomas, M. Daturi, H. Arnolds, D.A. King, Real-Time Infrared Detection of Cyanide Flip on Silver-Alumina NOx Removal Catalyst, Science 324 (2009) 1048–1051.
[58] S. Chansai, R. Burch, C. Hardacre, J. Breen, F. Meunier, The use of short time-on-stream in situ spectroscopic transient kinetic isotope techniques to investigate the mechanism of hydrocarbon selective catalytic reduction (HC-SCR) of NOx at low temperatures, J. Catal. 281 (2011) 98–105.